ORIGINAL RESEARCH

Lysosome-Associated Membrane Proteins (LAMP) Maintain Pancreatic Acinar Cell Homeostasis: LAMP-2–Deficient Mice Develop Pancreatitis

Olga A. Mareninova,[1,2,*] Matthias Sendler,[3,*] Sudarshan Ravi Malla,[3] Iskandar Yakubov,[2] Samuel W. French,[4] Elmira Tokhtaeva,[1,2] Olga Vagin,[1,2] Viola Oorschot,[5,6] Renate Lüllmann-Rauch,[7] Judith Blanz,[8] David Dawson,[2] Judith Klumperman,[5] Markus M. Lerch,[3] Julia Mayerle,[3] Ilya Gukovsky,[1,2] and Anna S. Gukovskaya[1,2]

[1]VA Greater Los Angeles Healthcare System; [2]David Geffen School of Medicine, University of California at Los Angeles, Los Angeles, California; [3]Department of Medicine A, University Medicine, Ernst-Moritz-Arndt University Greifswald, Greifswald, Germany; [4]Harbor-UCLA Medical Center, Torrance, CA; [5]University Medical Center Utrecht, Utrecht, the Netherlands; [6]Monash Micro Imaging, Monash University, Melbourne, Victoria, Australia; [7]Anatomical and [8]Biochemical Institute, Christian-Albrechts-University Kiel, Kiel, Germany

SUMMARY

Defective autophagy is increasingly implicated in the pathogenesis of pancreatitis. Here we show that lysosome-associated membrane proteins (LAMPs) are degraded in experimental and human pancreatitis; LAMP-2 maintains acinar cell homeostasis, and its genetic ablation causes impaired autophagy and spontaneous pancreatitis.

BACKGROUND & AIMS: The pathogenic mechanism of pancreatitis is poorly understood. Recent evidence implicates defective autophagy in pancreatitis responses; however, the pathways mediating impaired autophagy in pancreas remain largely unknown. Here, we investigate the role of lysosome associated membrane proteins (LAMPs) in pancreatitis.

METHODS: We analyzed changes in LAMPs in experimental models and human pancreatitis, and the underlying mechanisms: LAMP deglycosylation and degradation. LAMP cleavage by cathepsin B (CatB) was analyzed by mass spectrometry. We used mice deficient in LAMP-2 to assess its role in pancreatitis.

RESULTS: Pancreatic levels of LAMP-1 and LAMP-2 greatly decrease across various pancreatitis models and in human disease. Pancreatitis does not trigger the LAMPs' bulk deglycosylation but induces their degradation via CatB-mediated cleavage of the LAMP molecule close to the boundary between luminal and transmembrane domains. LAMP-2 null mice spontaneously develop pancreatitis that begins with acinar cell vacuolization due to impaired autophagic flux, and progresses to severe pancreas damage characterized by trypsinogen activation, macrophage-driven inflammation, and acinar cell death. LAMP-2 deficiency causes a decrease in pancreatic digestive enzymes content, and stimulates the basal and inhibits cholecystokinin-induced amylase secretion by acinar cells. The effects of LAMP-2 knockout and acute cerulein pancreatitis overlap, which corroborates the pathogenic role of LAMP decrease in experimental pancreatitis models.

CONCLUSIONS: The results indicate a critical role for LAMPs, particularly LAMP-2, in maintaining pancreatic acinar cell

homeostasis and provide evidence that defective lysosomal function, resulting in impaired autophagy, leads to pancreatitis. Mice with LAMP-2 deficiency present a novel genetic model of human pancreatitis caused by lysosomal/autophagic dysfunction. *(Cell Mol Gastroenterol Hepatol 2015;1:678–694; http://dx.doi.org/10.1016/j.jcmgh.2015.07.006)*

Pancreatitis is a potentially fatal disease with considerable morbidity and mortality, the pathogenesis of which remains obscure and for which no specific or effective treatment has been developed.[1,2] Accumulation of large vacuoles in acinar cells, the main exocrine pancreas cell type, is a long-noted but poorly understood feature of both experimental and human pancreatitis.[3–6] Evidence from the past several years indicates that these vacuoles are mostly autolysosomes, and their accumulation is a result of impaired autophagic flux.[6–9] Autophagy comprises several intracellular pathways of lysosome-mediated degradation and recycling of organelles, long-lived proteins, and lipids.[10–12] Its major pathway, macroautophagy (hereafter

referred to as *autophagy*) begins with the formation of autophagosomes that sequester material destined for degradation. Autophagosomes ultimately fuse with lysosomes, generating autolysosomes in which cargo is degraded by lysosomal hydrolases such as cathepsins.

Although autophagy is increasingly implicated in the mechanism of pancreatitis,[6–9,13] the pathways leading to its impairment in the pancreas remain largely unknown. Because autophagy is lysosome driven, one mechanism of impaired autophagic flux could be defective function of lysosomes. Lysosome-associated membrane proteins (LAMPs) play critical and diverse roles in the function of lysosomes.[14,15] LAMP-1 and LAMP-2 are heavily glycosylated proteins and major constituents of the glycoconjugate coat on the inside of the lysosomal membrane.[15,16] LAMPs protect the cytoplasm and the limiting lysosomal membrane itself from the action of acid hydrolases, and they regulate the fusion of lysosomes with other organelles (in particular autophagosomes), lysosomal proteolytic activity, and phagocytosis.[14,15,17–19] The LAMP-2a isoform acts as a specific translocation receptor in chaperone-mediated autophagy.[20] LAMP-2 deficiency in mice results in cardiomyopathy, representing a model of Danon disease.[14,18] Although vacuole accumulation has been reported in pancreas of LAMP-2 null mice,[18] the consequences of LAMP deficiency for exocrine pancreas have not been explored.

Here, we show that pancreatic levels of LAMP-1 and LAMP-2 proteins decrease across various experimental models of nonalcoholic and alcoholic pancreatitis, as well as in human disease. Our data, including mass spectrometry (MS), indicate that LAMPs' decrease in pancreatitis is caused by their degradation mediated by cathepsin B. We find that LAMP-2 null mice spontaneously develop pancreatitis and that LAMP-2 deficiency causes dysregulation of amylase secretion from acinar cells. The results indicate a critical role of lysosomal/autophagic pathways for the exocrine pancreas.

Materials and Methods
Experimental Pancreatitis

Acute cerulein (CR) pancreatitis was induced, as described elsewhere,[6,21–24] in male Sprague-Dawley rats and in C57BL/6 and LAMP-2 null mice of both sexes that received hourly intraperitoneal (IP) injections of 50 μg/kg CR; the controls received similar injections of physiologic saline. If not stated otherwise, rats were euthanized 4 hours and mice 7 hours after the first injection. L-Arginine (Arg) pancreatitis was induced in rats of both sexes by 2 hourly IP injections of 2.5 g/kg Arg; the controls received similar injections of saline.[6,22] The animals were euthanized 24 hours after the first injection. Choline-deficient, ethionine-supplemented (CDE) pancreatitis was induced in young ($\sim$5-weeks old) female mice fed either CDE or control diet.[6,22] Mice were euthanized 72 hours after initiation of the diet. Ethanol plus low-dose CR pancreatitis[25] was induced in rats that were fed for 6 weeks Lieber-DeCarli ethanol-containing diet and then received four hourly IP injections of either saline or low-dose (0.5 μg/kg) CR; this dose of CR does not induce pancreatitis responses in rats fed isocaloric control diet.

All experimental protocols were approved by animal research committees of VA Greater Los Angeles Healthcare System and Ernst-Moritz-Arndt-University (Greifswald, Germany), in accordance with U.S. National Institutes of Health guidelines.

Genetically Modified Mice

Mice deficient in LAMP-2, cathepsin B (CatB), or CatD have been described elsewhere.[14,15,18,23,26]

Human Pancreas Specimens

Samples of human normal pancreas and pancreatitis were evaluated for the presence of acinar compartment and provided deidentified by Pancreas Tissue Bank of the University of California at Los Angeles (UCLA) Department of Pathology (D.D.) according to a protocol approved by the UCLA institutional review board.

Isolation of Pancreatic Acinar Cells and Lobules

Pancreatic acinar cells were isolated from wild-type and LAMP-2 null mice using a standard collagenase digestion procedure[6,23] and maintained in Dulbecco's modified Eagle medium containing 2% bovine serum albumin, and 10 mM HEPES. Pancreatic lobules were prepared[27] by injecting into freshly dissected pancreas of a buffer consisting of (mM) 10 HEPES, 137 NaCl, 4.7 KCl, 0.56 $MgCl_2$, 1.28 $CaCl_2$, 0.6 Na_2HPO_4, 5.5 D-glucose, 2 L-glutamine, and essential amino acids solution. The buffer was supplemented with 0.1 mg/mL soybean trypsin inhibitor and 1 mg/mL bovine serum albumin, adjusted to pH 7.4, and gassed with 100% O_2. The lobules ($\sim$2-mm thick) were then excised and incubated at 37°C in 199 medium containing 0.1 mg/mL soybean trypsin inhibitor in the presence or absence of cholecystokinin (CCK) and other agents as indicated.

Preparation of Tissue and Cell Lysates, and Membrane and Cytosolic Fractions

Portions of frozen tissue or lobules were homogenized on ice in radioimmunoprecipitation assay buffer supplemented with 1 mM phenylmethylsulfonyl fluoride and protease inhibitors' cocktail. Supernatants were collected and stored at −80°C. Protein concentration in the supernatants was determined by Bradford assay (Bio-Rad Laboratories, Hercules, CA). To obtain cytosolic and membrane fractions, pancreatic tissue was homogenized in a buffer containing 25 mM Tris-HCl (pH 7.4), 150 mM NaCl, 1 mM $MgCl_2$, and protease inhibitor cocktail. Postnuclear supernatant was centrifuged for 2 hours at 150,000g, and both the pellet (membrane fraction) and supernatant (cytosolic fraction) were collected separately and used for the immunoblot analysis.

Preparation of Lysosome-Enriched Fraction

The pancreas was dissected, homogenized in four volumes of extraction buffer (5 mM MES, pH 7.0, 250 mM sucrose, 1 mM $MgSO_4$, and protease inhibitor cocktail) per gram of tissue, and the homogenate was centrifuged at 1000g for 10 minutes at 4°C. Postnuclear supernatant was

further centrifuged at 20,000g for 20 minutes at 4°C, and the pellet (crude lysosomal fraction) was collected, incubated with 8 mM $CaCl_2$ to precipitate mitochondria and endoplasmic reticulum, and then centrifuged at 5000g for 10 minutes. The lysosome-containing supernatant[28] was stored at −80°C. The absence of cyclooxygenase IV (COX IV) in the cytosolic and lysosome-enriched fractions, and lack of lactate dehydrogenase in the membrane fraction were used to evaluate the quality of subcellular fractionation and the degree of enrichment.

Immunoblot Analysis

Proteins in pancreatic tissue and cell homogenates or cytosolic and membrane fractions were separated by sodium dodecyl sulfate polyacrylamide gel electrophoresis (SDS-PAGE). Blots were developed for visualization using enhanced chemiluminescence detection kit (Pierce Biotechnology, Rockford, IL); band intensities were quantified by densitometry using the FluorChem HD2 imaging system (Alpha Innotech/ProteinSimple, San Jose, CA).

Antibodies

We used Abs against the C-terminal region of rat and mouse LAMP-1 (ab24170; Abcam, Cambridge, MA), LAMP-2 (L0668; Sigma-Aldrich, St. Louis, MO), LAMP-2a (51-2200; Invitrogen/Life Technologies, Carlsbad, CA), and lysosomal integral membrane protein type-2 (LIMP-2) (NB400-129; Novus Biologicals Oakville, ON, Canada); and against full-length/luminal mouse LAMP-1 (1d4b; Iowa Developmental Studies Hybridoma Bank, University of Iowa, Iowa City, IA), and mouse LAMP-2 (GL2A7; Iowa Developmental Studies Hybridoma Bank). The following Abs were used for immunofluorescence and immunohistochemical analyses: collagen-1 (ab292; Abcam), Ki67 (IHC-00375; Bethyl Laboratories, Inc. Montgomery, TX), α-smooth muscle actin (α-SMA) (clone 1A4; Sigma-Aldrich), insulin (4590; Cell Signaling Technology, Beverly, MA), CD68 (ABIN181836; Antibodies Online, Atlanta, GA), and CD206 (OASA05048; Aviva Systems Biology, San Diego, CA).

Light and Fluorescence Microscopy

Histochemical staining (H&E, Goldner trichrome) and immunostaining for α-SMA, collagen-1, Ki67, LAMPs, and CatD was performed on paraffin-embedded pancreas tissue sections using Target Retrieval buffer (Dako, Carpinteria, CA). Immunostaining for macrophages (CD68 and CD206) was performed on cryosections. Images were acquired with a Nikon Eclipse TE2000-S microscope (Nikon Instruments, Melville, NY) equipped with a charge-coupled device (CCD) camera, using the SPOT imaging software (SPOT Imaging Solutions, Sterling Heights, MI), or with a Zeiss LSM 710 confocal microscope using 63× objective (Carl Zeiss Light Microscopy, Göttingen, Germany). Nuclei were counterstained with 4′,6-diamidino-2-phenylindole (DAPI). To determine the percentage of colocalization of two proteins, images obtained with the use of corresponding antibodies were loaded into the ImageJ software (http://imagej.nih.gov/ij/); the ratios of green (fluorescein isothiocyanate conjugated secondary antibody) or red (Texas Red conjugated secondary antibody) cells to merged cells were determined using the colocalization plug-in. The quantification of immunohistochemical images was performed as described by Sendler et al.[24]

Transmission Electron Microscopy and Immunogold Electron Microscopy

The tissue was cut into 1-mm cubes and fixed at 4°C in 2.5% glutaraldehyde in 0.15 M sodium cacodylate (pH 7.4) overnight. After fixation in 1% OsO_4 followed by uranyl acetate, tissue was dehydrated in ethanol and embedded in epoxy resin. We examined 100-nm-thick sections in a Hitachi-600 electron microscope (Hitachi High Technologies America, Schaumburg, IL). For Immunogold EM (electron microscopy), the rats were perfused with either 2% wt/vol paraformaldehyde (PFA) in 0.1 M phosphate buffer (pH 7.4) or 2% wt/vol PFA, 0.2% wt/vol glutaraldehyde in 0.1 M phosphate buffer, pH 7.4. After the perfusion fixation with 2% PFA, the tissues were removed and immediately immersed in 4% wt/vol PFA in 0.1 M phosphate buffer and kept overnight at 4°C.

The fixed tissues were further processed for cryosectioning and Immunogold EM as described elsewhere.[29] In brief, ultrathin cryosectioning was performed at −120°C in a Leica UCT-FCS ultracryomicrotome (Leica Microsystems, Buffalo Grove, IL). The sections were transferred to copper grids by pickup with a 1:1 mixture of 2.3 M sucrose in phosphate-buffered saline (PBS) and 2% wt/vol methyl cellulose. The grids were incubated first on 2% gelatin/PBS at 37°C, blocked with 0.02 M glycine/PBS and 1% bovine serum albumin/PBS, and subsequently incubated with primary antibodies followed by protein A-gold (Cell Microscopy Centre, UMC Utrecht, the Netherlands). The sections were contrasted with 2% uranyl acetate/oxalate.

Glycosidase Treatment

Proteins in pancreatic membrane fractions were denatured by incubation at 80°C for 5 minutes in the presence of 0.5% sodium dodecyl sulfate, and then treated with peptide:N-glycosidase (PNGase) F from *Flavobacterium meningosepticum* (New England BioLabs, Ipswich, MA) or with endonuclease H from *Streptomyces plicatus* (Glyko, ProZyme, Hayward, CA) at 37°C for 1 or 3 hours, respectively, according to the manufacturers' protocols. Incubation with Jack bean α-mannosidase (Sigma-Aldrich) was performed in 25 mM sodium acetate buffer (pH 5.0) containing 1% Triton X-100 at 37°C for 3 hours.

Cleavage of rLAMP-1 by CatB

Before use, recombinant mouse CatB (R&D Systems, Minneapolis, MN) was activated by 30 minutes of incubation with 1 mM dithiothreitol on ice. CatB-induced conversion of trypsinogen (Sigma-Aldrich) to trypsin[6] served as a positive control for its full activity. Recombinant mouse LAMP-1 (rLAMP-1, 2 μg/mL; R&D Systems) was incubated with activated CatB in 25 mM MES, 2 mM dithiothreitol, pH 5.0, for 1 hour at 30°C, and changes in rLAMP-1 level were measured by immunoblot. The rLAMP-1 peptides generated

by incubation with CatB were identified by tandem MS (Stanford University Mass Spectrometry Core) using an LTQ Orbitrap Velos MS (Thermo Fisher Scientific, Waltham, MA) set in high-high data-dependent mode to fragment, via higher energy collisional dissociation (HCD), the top eight most intense precursor ions. The data were analyzed both manually and by Sequest on a Sorcerer station (Sage-N Research, Seattle, WA).

Pancreatitis Parameters

Serum amylase was measured in a Hitachi 707 analyzer (Antech Diagnostics, Irvine, CA). *Trypsin activity* was measured in tissue and cell homogenates, as described elsewhere,[6,23,24,26] using specific fluorogenic substrate Boc-Gln-Ala-Arg-AMC (Sigma-Aldrich) or R110-Ile-Pro-Arg (Invitrogen/Life Technologies). Trypsin activity in each sample was determined using a standard curve for purified trypsin (Worthington Biochemical, Lakewood, NJ). To measure the total amount of trypsinogen, the homogenate was incubated with 0.2% (wt/vol) enterokinase in 100 mM Tris-HCl buffer (pH 8.0; 37°C; 1 hour) to convert all trypsinogen to trypsin, followed by measurement of trypsin activity.

Myeloperoxidase (MPO) activity was measured as described elsewhere.[24] Pancreatic tissue was homogenized on ice in 20 mM potassium phosphate buffer (pH 7.4) and centrifuged at 4°C. The pellet was resuspended in 50 mM potassium phosphate buffer (pH 6.0) containing 0.5% cetyltrimethyl ammonium bromide, 10 mM phenylmethylsulfonyl fluoride, and 10 μM soybean trypsin inhibitor. The suspension was freeze-thawed in cycles, sonicated, and centrifuged at 20,000g and 4°C. MPO activity was assayed in 50 mM potassium phosphate buffer (pH 6.0) containing 0.53 mM *O*-dianisidine and 0.15 mM H_2O_2. The initial increase in absorbance was measured at 30°C in a SpectraMax spectrophotometer (Molecular Devices, Sunnyvale, CA). The results are expressed in units of MPO activity per total protein, using purified MPO (Calbiochem/EMD Millipore, San Diego, CA) as a standard.

Caspase-3 activity was measured in pancreatic tissue homogenates by a fluorometric assay using R110-DEVD substrate (Invitrogen/Life Technologies). Amylase release was measured from acinar cells incubated for 30 minutes with and without CCK-8 at various concentrations. Values are the ratio between the amount of amylase released into the medium [measured with a photometric assay (Roche-Hitachi, Rotkreuz. Switzerland)] and the total cellular amylase determined by permeabilizing cells with 1% Triton X-100.

Acinar cell vacuolization, necrosis, apoptosis, and inflammatory cell infiltration were quantified on H&E stained pancreatic tissue sections. At least 1000 acinar cells/mouse were analyzed on several high-power fields. Necrosis was measured either as percentage of necrotic cells/100 acinar cells or graded on 0–4 scale on 400× high-power fields. Apoptosis was measured with a terminal deoxynucleotidyl transferase–mediated deoxyuridine triphosphate nick-end labeling (TUNEL) assay (Promega, Madison, WI). Macrophages were further quantified by immunostaining for CD68 and CD206 markers; chloroacetate esterase staining was used for neutrophils.

Statistical Analysis

Data are expressed as mean $\pm$ standard error of the mean (SEM). Statistical analysis was performed on Prism 5 software (GraphPad Software, San Diego, CA), using two-tailed, unpaired Student t test for comparisons between two groups. $P < .05$ was considered statistically significant.

Results

LAMP-1 and LAMP-2 Decrease in Experimental and Human Pancreatitis

Immunoblot analysis (Figure 1*A* and *B* and Figure 2*A–C*) showed a pronounced decrease in pancreatic levels of LAMP-1 and LAMP-2 in five dissimilar rat and mouse models of acute pancreatitis, namely, those induced by administration of supramaximal CR (analog of CCK-8) or L-arginine (Arg); by CDE diet; or by ethanol feeding combined with low-dose CR (see *Materials and Methods*). Ethanol feeding alone caused some decrease in pancreatic LAMPs, but much less than in ethanol + low-dose CR pancreatitis (Figure 1*A*). Pancreatitis-induced decreases were observed for LAMP isoforms mediating macroautophagy and for LAMP-2a, the isoform mediating chaperone-mediated autophagy; however, there was no effect on LIMP-2, a member of another family of lysosomal membrane proteins (Figure 2*A–C*). The down-regulation of LAMPs occurred early in the course of pancreatitis; it was already prominent at 30 minutes after induction of CR pancreatitis (Figure 1*A*).

Immunogold-EM localized LAMPs in normal pancreas to acinar cell lysosomes and autolysosomes (Figure 1*C*). Accordingly, immunofluorescence showed punctate LAMP staining in acinar cells of normal human (Figure 1*D*) and rat (Figure 2*D*) pancreas. Although LAMPs retained their lysosomal/autolysosomal localization in pancreatitis (Figure 1*C*), the number of LAMP puncta greatly decreased in both human (Figure 1*D*) and experimental (Figure 2*D*) pancreatitis, in accord with the immunoblot data. Notably, immunolabeling for the lysosomal marker CatD was not affected in either human or experimental pancreatitis (Figure 1*D* and Figure 2*D*). However, the extent of CatD colocalization with LAMP-2 was markedly reduced in pancreatitis (Figure 1*D* and *E;* Figure 2*D* and *E*), indicating a selective LAMP decrease in lysosomes. This conclusion is supported by immunoblot analysis (Figure 2*B* and *C*; and data not shown) showing that 1) in both control and diseased pancreas, LAMPs were only present in the membrane but not cytosolic fractions; 2) pancreatitis decreased LAMP levels in membrane fractions and in lysosome enriched fraction; and 3) pancreatitis had much less effect on LIMP-2, including in the lysosome-enriched fraction.

Pancreatitis Preferentially Affects LAMPs C Terminus

The LAMP molecule is composed of a large luminal ectodomain, the transmembrane domain, and a very small (11 aa) C-terminal cytoplasmic tail.[14–17] We observed that the extent of the LAMP decrease in pancreatitis was different in immunoblots obtained on the same samples using Abs against LAMP C terminus versus Abs that
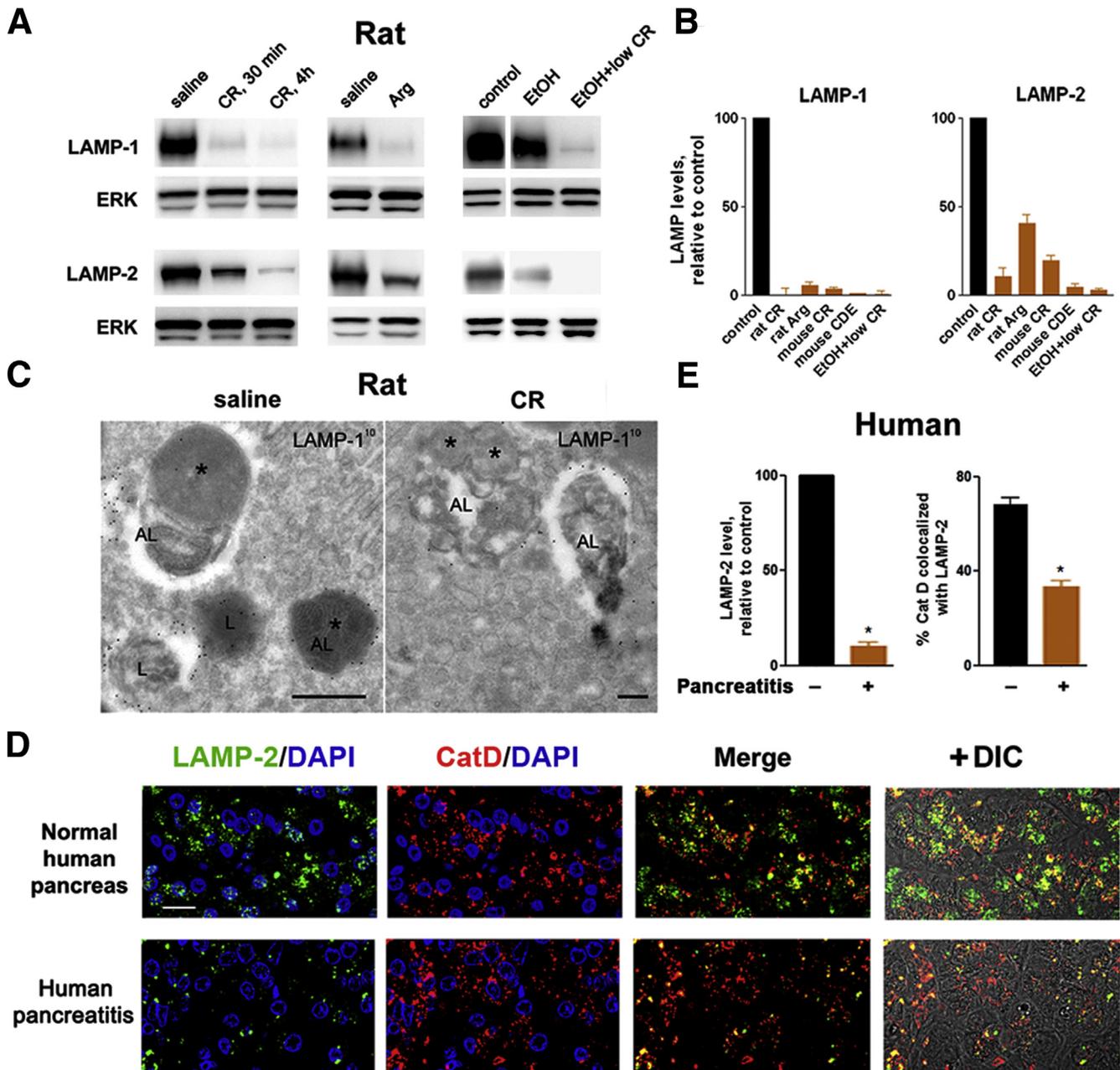
Figure 1. Pancreatic levels of lysosome-associated membrane protein 1 (LAMP-1) and LAMP-2 decrease in rodent models and human pancreatitis. Pancreatitis was induced in rats by administration of cerulein (CR) or L-arginine (Arg), or by a combination of ethanol diet (EtOH) and low-dose CR; and in mice, by CR or feeding choline-deficient ethionine supplemented (CDE) diet (see *Materials and Methods*). (*A*, *B*). Immunoblot analysis of pancreatic LAMP levels in fully developed pancreatitis and at the onset (after 30 minutes) of CR pancreatitis, using Abs against the C terminus of LAMP-1 (Abcam) and LAMP-2 (Sigma). In this and other figures, extracellular signal-activated kinases 1/2 (ERK1/2), β-actin, or glyceraldehyde-3-phosphate dehydrogenase (GAPDH) are loading controls; each lane represents an individual animal; the data are representative of several immunoblots from at least three animals for each condition; the narrow white space on the immunoblot indicates that the lanes are on the same blot but not contiguous. (*B*) The densitometric intensity of LAMP band was normalized to that of ERK in the same sample, and the mean LAMP/ERK ratio in pancreatitis group was further normalized to that in control group. Values are mean ± SEM (n = 4 per group). (*C*). Immunogold electron microscopy labeling shows LAMP-1 in lysosomes (L) and autolysosomes (AL) in pancreas of rats with CR pancreatitis and control (saline). The asterisks point to remnants of sequestered organelles. Scale bar: 500 nm. (*D, E*). Immunofluorescence analysis of LAMP-2 (using the C-terminal Ab) and cathepsin D (CatD) in human pancreas. Nuclei staining with 4′,6-diamidino-2-phenylindole (DAPI) (*blue*; not shown in "merge" panels). DIC, differential interference contrast, which prominently displays zymogen granules area in acinar cells. Scale bar: 10 μm (all images). (*E*) LAMP-2 punctate staining and colocalization of CatD with LAMP-2 in human normal pancreas and pancreatitis were quantified with ImageJ. Values are mean ± SEM from four normal and seven pancreatitis tissue samples from different patients. *P < .05 versus normal pancreas.
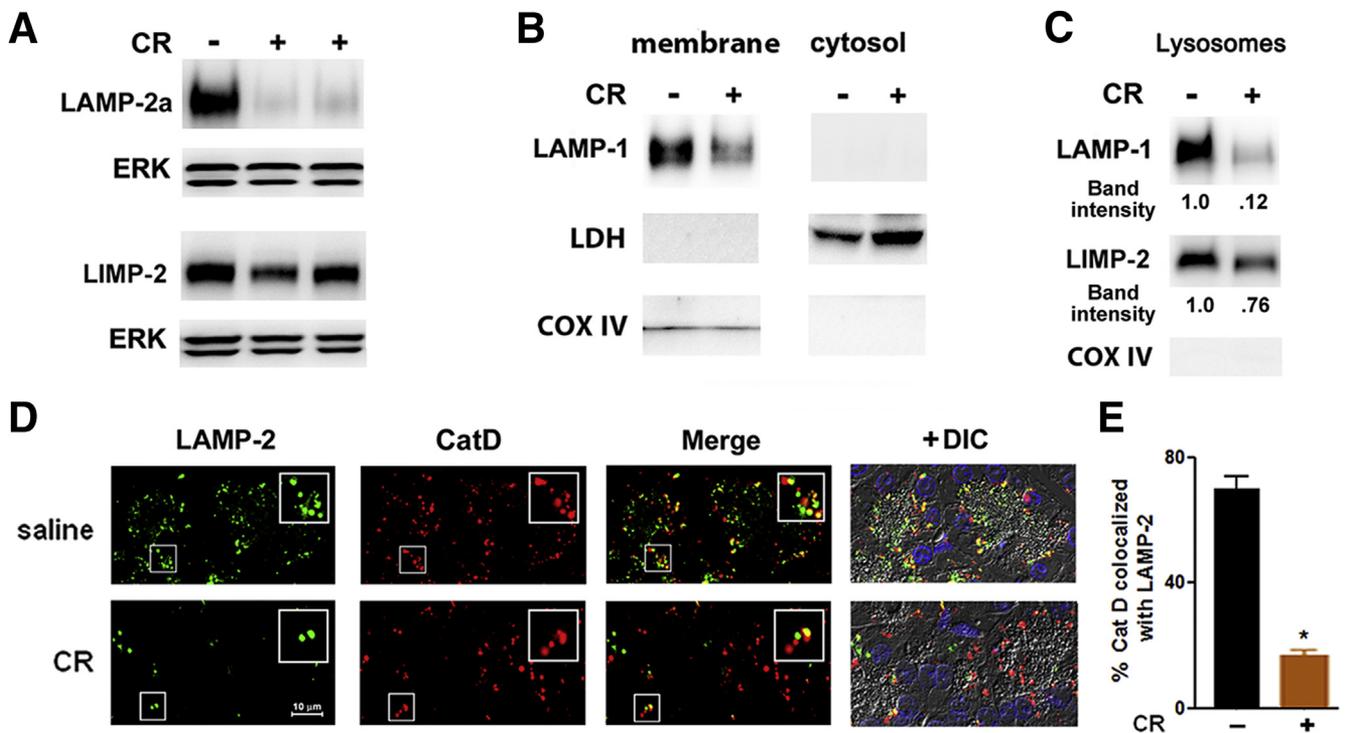
Figure 2. Experimental pancreatitis causes a decrease in lysosome-associated membrane proteins (LAMPs), including LAMP-2a, but not in lysosomal integral membrane protein type-2 (LIMP-2). Cerulein (CR) pancreatitis was induced in mice (*A–C*) and rats (*D*). Pancreatic levels of indicated proteins were measured by immunoblot, using C-terminal Abs, in (*A*) whole tissue homogenates, (*B*) membrane and cytosolic fractions, and (*C*) lysosome-enriched fraction (see *Materials and Methods*). Extracellular signal-activated kinases 1/2 (ERK1/2), lactate dehydrogenase, and cyclooxygenase IV (COX IV) served as controls for equal loading and the quality of subcellular fractionation. Data in *B* and *C* are representative of two independent experiments, with similar results. (*D*) Colocalization of LAMP-2 and cathepsin D (CatD) in pancreas of control (saline) rats and rats with CR pancreatitis. Tissue sections were double immunostained for LAMP-2 (using C-terminal Ab) and CatD. Insets show higher magnification for the areas in smaller boxes. Scale bar is the same for all images. DIC, differential interference contrast. (*E*). CatD colocalization with LAMP-2 was quantified with ImageJ. Values are mean ± SEM (n = 3–4 per group); *P < .05 versus control.

recognize the luminal part of the LAMP molecule (Figure 3). In control pancreas, both types of antibodies showed LAMP bands of similar intensity (Figure 3*A* and *B*). This was not the case in pancreatitis models: pancreatitis-induced decreases in LAMP-1 and LAMP-2 were much greater with C-terminal Abs than with Abs against LAMP luminal part (Figure 3*A–C*). Compared with whole tissue, these differences were even more pronounced in lysosome-enriched fraction (Figure 3*D*). Moreover, a slight shift in the position of LAMP band recognized by the two types of Abs was observed in pancreatitis samples on some immunoblots, as illustrated in Figure 3*D*. These results indicate that pancreatitis preferentially affects LAMP C terminus so that LAMPs cease to be recognizable by C-terminal Abs.

Pancreatitis Does Not Cause Bulk LAMP Deglycosylation

A logical explanation for the observed preferential effect on the LAMP C terminus is that pancreatitis causes the degradation of LAMPs. One possible underlying mechanism could be LAMP deglycosylation, which decreases the stability of LAMP-1 and LAMP-2 proteins.[30] However, our results (Figure 4) argue against such possibility. In both controls and pancreatitis, immunoblot with either C-terminal or luminal Abs did not show the lower molecular mass LAMP bands indicative of accumulation of under- or deglycosylated molecules (Figure 4*A* and *B*). Complete deglycosylation of samples with peptide:N-glycosidase (PNGase) F produced bands corresponding to deglycosylated LAMPs (~50 kDa), but it did not eliminate the difference between pancreatitis and control (Figure 4*A* and *B*). Of note, our data show that the Abs against the luminal part of LAMPs (from Iowa Developmental Studies Hybridoma Bank) do not recognize deglycosylated LAMPs, but the C-terminal Abs do (Figure 4*A* and *B*). Thus, the fact that in pancreatitis there is more LAMP immunoreactivity detected with the luminal Abs than with the C-terminal Abs (Figure 3) indicates that pancreatitis-induced decreases in LAMP-1 and LAMP-2 are not due to their deglycosylation.

To determine whether LAMPs in pancreatitis are present as fully mature glycans, we treated control and pancreatitis samples with endoglycosidase H or Jack bean α-mannosidase, which cleave partially processed but not fully mature glycans.[31] LAMPs were insensitive to the action of these enzymes (Figure 4*A*), indicating fully mature
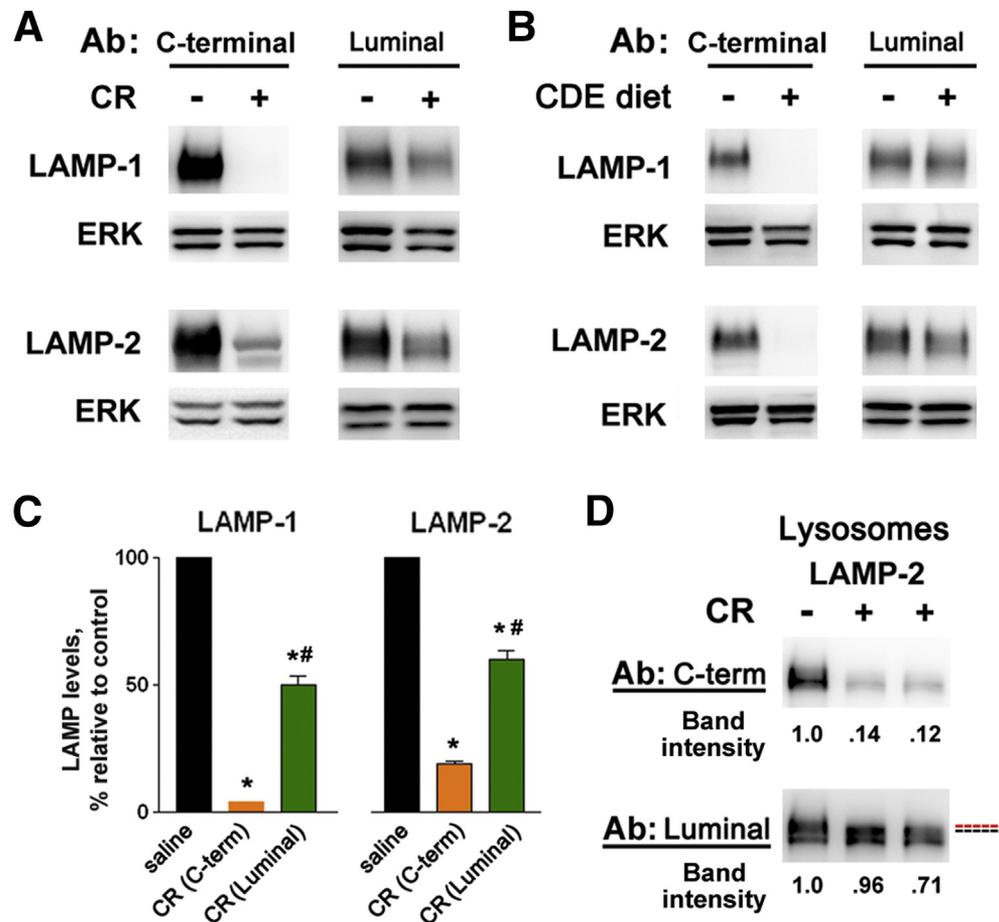
Figure 3. Pancreatitis preferentially affects lysosome-associated membrane protein (LAMP) C terminus. LAMP levels were measured by immunoblot in (*A–C*) whole-tissue homogenates and (*D*) lysosome-enriched fraction from pancreata of mice with cerulein (CR) or choline-deficient, ethionine-supplemented diet (CDE) pancreatitis, using either Abs against the C terminus of LAMP-1 (Abcam) and LAMP-2 (Sigma-Aldrich) or Abs that recognize the luminal part of LAMPs (Iowa Developmental Studies Hybridoma Bank; see *Materials and Methods*). (*C*) LAMP band intensity was normalized to that of extracellular signal-activated kinases (ERK) in the same sample, and the mean LAMP/ERK ratio in pancreatitis group was further normalized to that in control (saline) group. Values are mean ± SEM (n = 4 per group). *$P < .05$ versus control; #$P < .05$ versus the corresponding LAMP band intensity detected with C-terminal Ab. (*D*) Red and blue dashed lines indicate a shift in the position of LAMP-2 band.

(complex-type) LAMP glycosylation in both control and pancreatitis. Also, there was no detectable shift in LAMP-2 electrophoretic mobility upon treatment of either control or pancreatitis samples with neuraminidase (Figure 4*C*), indicating no or very few terminal sialic acid residues in LAMP-2. However, there was a slight shift in the electrophoretic mobility upon treatment with neuraminidase + *O*-glycanase (Figure 4*C*), indicating the presence of *O*-glycans.

Cathepsin B Mediates the LAMP Decrease in Pancreatitis

We next considered another possible mechanism of LAMP degradation: their cleavage by lysosomal proteases. Such a mechanism, regulating chaperone-mediated autophagy, was shown for LAMP-2a cleavage by CatA.[32,33] The luminal part of LAMPs is largely protected against lysosomal proteases by being heavily glycosylated; however, a short

region near the boundary with the transmembrane domain is less glycosylated and thus could be prone to proteolytic cleavage in pathologic conditions (see below).

We specifically tested whether CatB could be involved in LAMP degradation in pancreatitis. This cysteine protease is important for pancreatitis because it mediates key pathologic responses of this disease: the inappropriate, intra-acinar trypsinogen activation and necrosis.[6,23,26,34] Pharmacologic inhibition and genetic ablation of CatB markedly ameliorate experimental pancreatitis.[23,26,34] However, it is not known whether CatB has pathologic actions other than trypsinogen activation.

We first measured the effects of E-64d, a broad-spectrum cysteine protease inhibitor, and CA-074Me, a selective CatB inhibitor, on LAMP levels. For this, we used an ex vivo model of pancreatitis,[6,23] namely, pancreatic lobules hyperstimulated with CCK-8. Both inhibitors largely prevented pancreatitis-induced decreases in LAMP-1 and
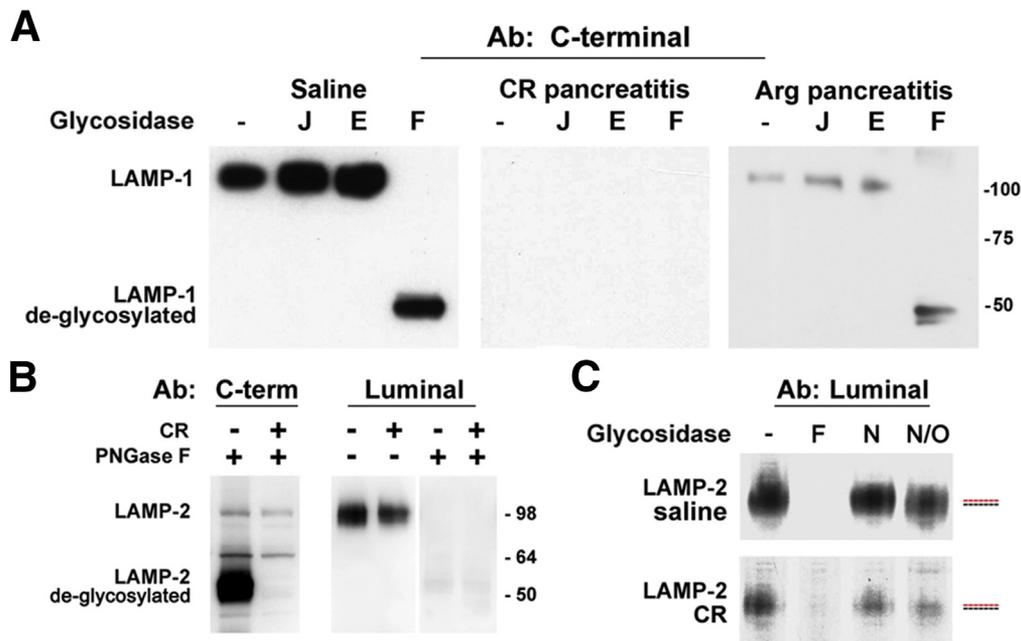
Figure 4. Pancreatitis does not cause bulk lysosome-associated membrane protein (LAMP) deglycosylation. Cerulein (CR) and L-arginine (Arg) pancreatitis were induced in (A) rats or (B, C) mice. Pancreatic tissue homogenates from control (saline) and pancreatitic animals were treated with PNGase F (F), Jack bean α-mannosidase (J), endoglycosidase H (E), neuraminidase (N), or neuraminidase plus O-glycanase (N/O), as described in *Materials and Methods*. LAMP-1 and LAMP-2 were analyzed by immunoblot using C-terminal or luminal Abs, as indicated. Numbers to the right are protein molecular mass markers in kDa. (C) Red and blue dashed lines indicate a shift in the position of LAMP-2 band.

LAMP-2 (Figure 5A and B; and data not shown). Differently, the irreversible serine protease inhibitor AEBSF [4-(2-aminoethyl)benzenesulfonyl fluoride] failed to prevent the CCK-induced LAMP decrease (Figure 5C) although it completely abrogated CCK-induced trypsinogen activation (Figure 5D), as previously reported elsewhere.[35] Thus, the CCK/CR-induced LAMP decrease is not mediated by trypsin.

In vivo, we further found (Figure 5E) that in mice deficient in CatB, CR pancreatitis caused essentially no decrease in LAMPs. Differently, pancreatitis-induced decreases in LAMPs were not abrogated by genetic ablation of another cathepsin, CatD (Figure 5F). Interestingly, the basal pancreatic LAMP levels were up-regulated in CatD$^{-/-}$ mice (Figure 5F).

Finally, we assessed whether CatB could directly cleave LAMPs. Incubation of recombinant mouse LAMP-1 (rLAMP-1) with active recombinant CatB caused a pronounced decrease in the rLAMP-1 level (Figure 6A). The decrease was much greater when detected with an Ab against C-terminal 6His-tag [substituting for the transmembrane and cytosolic domains (Met371–Ile406) in rLAMP-1; Figure 6E] than with the luminal Ab (Figure 6A). There was no decrease in rLAMP-1 when rCatB was omitted from the incubation mix. Mass spectrometric analysis (see *Materials and Methods*) showed that CatB cleaves LAMP-1 at several sites close to the boundary between the luminal and the transmembrane domains (Figure 6B–E). Of note, the cleavage site-predicting Web tool we used[36] identifies more than 20 potential (>95% specific) sites for CatB cleavage in LAMP-1, spread all over the luminal part of the molecule

(not shown). However, only a few of those were detected by MS in our in vitro assay, all clustered in a short region close to the transmembrane domain (Figure 6B–E). This region (c. Leu339 to Asn370 in LAMP-1) could, therefore, be susceptible to cleavage in pancreatitis; it is less glycosylated than the rest of the LAMPs luminal ectodomain. Interestingly, the cleavage of LAMP-2a by CatA also occurs in this region, at a site near the boundary between the luminal and transmembrane domains.[33]

LAMP-2 Deficiency Causes Spontaneous Pancreatitis

To assess the consequences of the LAMP decrease and elucidate the role of LAMP-2 in acinar cell homeostasis, we characterized in detail the exocrine pancreas damage in LAMP-2 null mice. We find that these mice[14,18] progressively develop histopathologic changes characteristic of pancreatitis (Figure 7A). Accumulation in acinar cells of abnormally large autolysosomes, seen with both light and electron microscopy, was the earliest manifestation of pancreatic damage, already prominent in 1-month-old LAMP-2 null mice (Figure 7A and F). Different from acinar cells, there was no vacuole accumulation or other histologic abnormalities in islets (Figure 7B). In accord with histology, LAMP-2 deficiency did not increase the blood glucose (Figure 7C), indicating little effect on the endocrine compartment. Acinar cell vacuolization (Figure 7 A,F) in the LAMP-2 null pancreas was associated with increases in microtubule-associated protein-1 light chain 3-II (LC3-II), an autophagy marker that uniquely
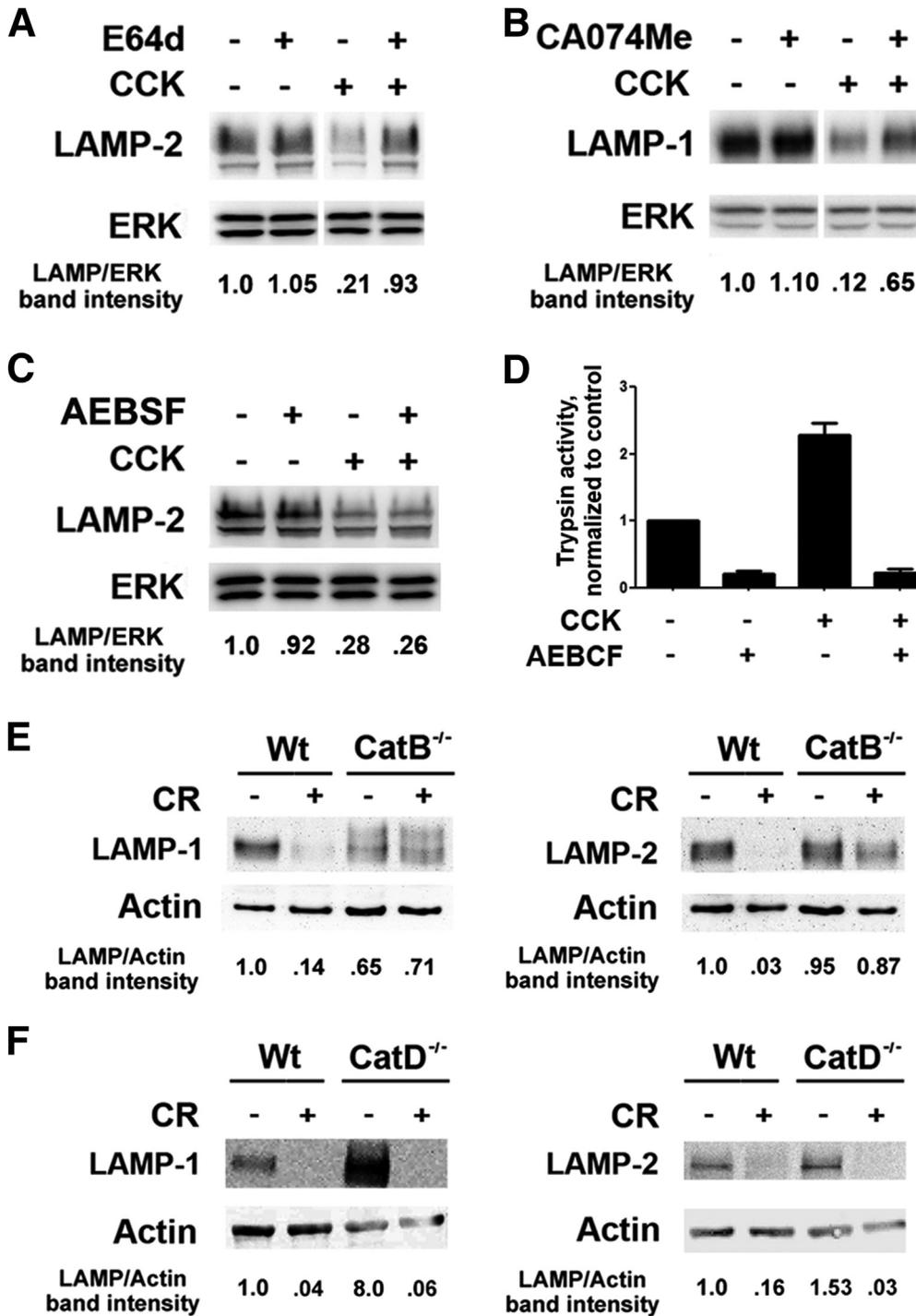
Figure 5. Lysosome-associated membrane protein (LAMP) degradation in cerulein (CR) pancreatitis is mediated by cathepsin B (CatB). LAMP levels were measured by immunoblot, using C-terminal Ab, in (A–C) freshly prepared pancreatic lobules incubated with or without 100 nM cholecystokinin-8 (CCK-8) in the absence and presence of (A) a broad-spectrum cysteine protease inhibitor E64d (50 μM), (B) CatB inhibitor CA074Me (50 μM), or (C) serine protease inhibitor AEBSF [4-(2-aminoethyl) benzenesulfonyl fluoride] (1 mM); and (E, F) in the pancreas of wild type, CatB$^{-/-}$, or CatD$^{-/-}$ mice with CR pancreatitis. LAMP band intensity was normalized to that of extracellular signal-activated kinase (ERK) or actin in the same sample. The data are representative of several immunoblots on at least three preparations of lobules or three mice of each genotype. (D). Trypsin activity was measured in mouse acinar cells incubated for 30 minutes with or without 100 nM CCK-8 in the absence and presence of 1 mM AEBSF. Values are mean $\pm$ SEM from duplicate measurements in two independent experiments.

localizes to autophagosomal membranes,[11,12,37,38] and p62/SQSTM1 (sequestosome 1), a protein that is degraded through autophagy[37–39] (Figure 7E). [Of note, the absence of LAMP-2 in the pancreas of LAMP-2 null mice was demonstrated with the C-terminal Ab (Figure 7D), validating the specificity of this Ab.]

Accumulation of enlarged autophagic vacuoles containing partially degraded cargo (in particular, remnants of organelles), and the increases in both LC3-II and p62 indicate defective autophagic flux.[10–12,38] These manifestations of impaired autophagy in LAMP-2 null pancreas are similar to those observed in wild-type pancreatitis (Figure 7E).[6,8]

Early acinar cell vacuolization in LAMP-2 null mice was followed by other pathologic responses of pancreatitis: tissue disorganization (Figure 7A), necrotic and apoptotic acinar cell death (Figure 8A and B) associated with compensatory proliferation (immunohistochemistry for Ki67; Figure 8B and C), and the intrapancreatic trypsinogen
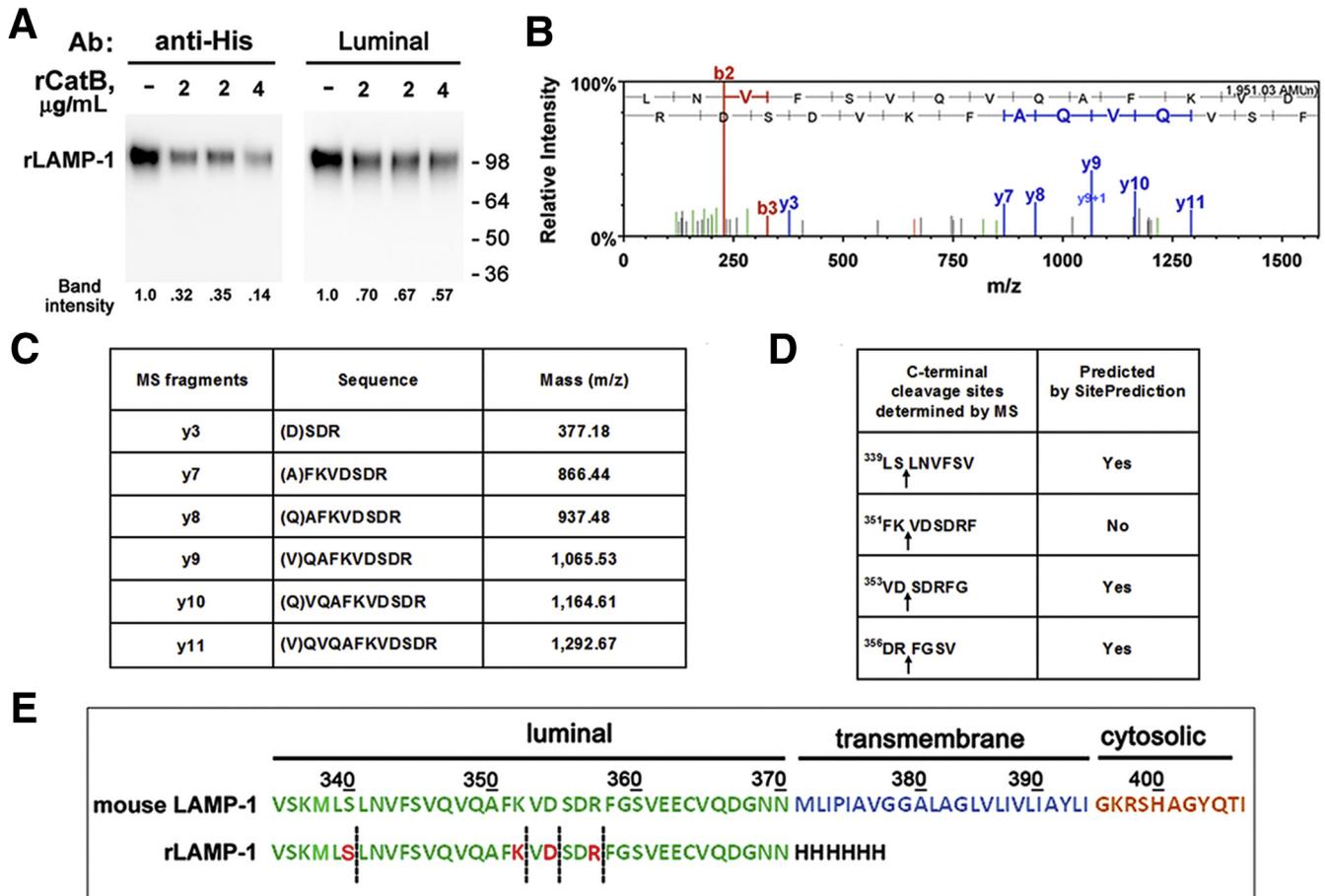
Figure 6. Mass spectrometry (MS) analysis of mouse recombinant lysosome-associated membrane protein 1 (LAMP-1) peptides generated by cleavage with cathepsin B (CatB). (*A*). Recombinant (r) mouse LAMP-1 (rLAMP-1) was incubated for 1 hour at 37°C with the indicated concentrations of active rCatB (see *Materials and Methods*). The rLAMP-1 level was measured by immunoblot using either the luminal Ab or an Ab against C-terminal 6-His tag; rLAMP-1 band intensity was normalized to that in the absence of rCatB. Numbers to the right are protein molecular mass markers in kDa. Representative of two independent experiments, with similar results. (*B, C*). Mass spectrometry data for C-terminal fragments of rLAMP-1 generated by incubation with CatB. (*D*). Comparison of CatB cleavage sites detected by MS versus CatB cleavage sites in mouse LAMP-1 predicted by the SitePrediction web tool (http://www.dmbr.ugent.be/prx/bioit2). (*E*). C-terminal amino acid sequences of mouse LAMP-1 and rLAMP-1. Dashed lines indicate sites of rLAMP-1 cleavage by CatB detected by MS.

activation (Figure 8B). LAMP-2 deficiency caused progressive increase in inflammatory cell infiltration (Figure 8A), which was predominantly macrophage but not neutrophil, driven (Figure 9A–C), a characteristic of chronic pancreatitis. As shown by immunostaining for CD68, a pan-macrophage/monocyte marker, and CD206, a marker of M2a macrophages, LAMP-2 deficiency stimulated infiltration of both proinflammatory M1 and profibrogenic M2 macrophages,[40] with the former predominant (Figure 9A). Immunohistochemical and immunoblot analyses showed significant up-regulation of α-SMA, a marker of activated stellate cells (Figure 9D, F, and G); however, there was no increase in fibrosis, as evidenced by lack of positive tri-chrome and collagen-1 staining (Figure 9D, E, and G). One possible explanation is that LAMP-2 deficiency blocks autophagy in stellate cells, resulting in their failure to produce extracellular matrix proteins. Indeed, loss of auto-phagic function in hepatic stellate cells was recently shown to reduce liver fibrogenesis.[41]

LAMP-2 Maintains Pancreatic Acinar Cell Homeostasis

LAMP-2 deficiency caused a marked decrease in digestive enzymes' pancreatic content, measured in both tissue and isolated acinar cells (Figure 10A, D, and F). In particular, amylase content decreased by ∼60%, which translated into an approximately twofold increase in amylase release into the circulation (although the absolute level of serum amylase did not change; Figure 10B and C). Furthermore, there was a ∼50% decrease in the average number of zymogen granules per acinar cell in LAMP-2 null pancreas (Figure 10D).

It is well established[34] that physiologic CCK concentrations stimulate, whereas its supramaximal concentrations inhibit, amylase release from acinar cells, producing the hallmark biphasic secretory response (Figure 10G and H). We found that in LAMP-2 null acinar cells the basal (unstimulated) amylase release was greater than in the wild type (Figure 10G) and the CCK-induced amylase release was
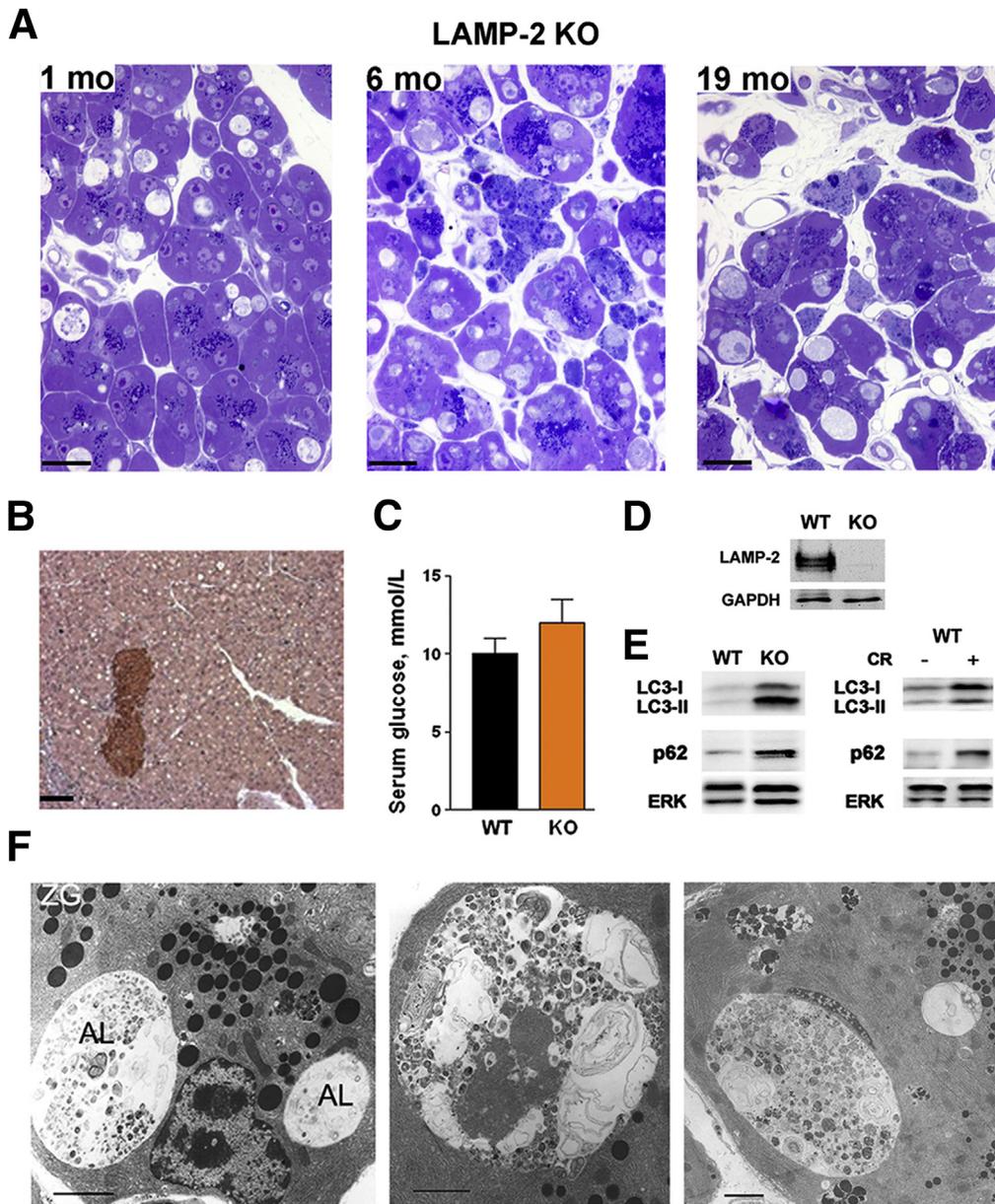
Figure 7. Lysosome-associated membrane protein 2 (LAMP-2) genetic ablation causes impaired autophagy in the exocrine pancreas. (A). Toluidine-blue stained pancreatic tissue sections from LAMP-2 null (knock-out) mice showing acinar cell vacuolization, tissue disorganization, and inflammatory cell infiltration. Scale bar: 20 μm. (B) Immunohistochemistry for insulin in pancreas of LAMP-2 knockout mice. Note massive vacuolization of acinar but not islet cells. Scale bar: 50 μm. (C). Serum glucose levels in wild-type and LAMP-2 knockout mice. Values are mean $\pm$ SEM (n = 3 per group). (D, E). LAMP-2, microtubule-associated protein-1 light chain 3 (LC3), and p62/SQSTM1 (sequestosome 1) were measured by immunoblot in pancreata of LAMP-2 knockout mice and wild-type mice with CR pancreatitis. (F). Electron micrographs showing abnormally large autolysosomes (AL) containing partially degraded material in pancreas of LAMP-2 knockout mice. ZG, zymogen granules. Scale bar: 2 μm. The data in B–F are for 6-month-old LAMP-2 knockout mice.

markedly inhibited (Figure 10H). Importantly, the inhibition was at both physiologic and supramaximal CCK concentrations. The results in Figure 10 indicate a critical role for LAMP-2 in regulating digestive enzyme secretion, the main function of acinar cells.

Effects of LAMP-2 Genetic Ablation on Acute Cerulein Pancreatitis

We next asked whether LAMP-2 deficiency affects the classic acute CR pancreatitis model. Histopathologic manifestations of CR pancreatitis in LAMP-2 null mice (tissue disorganization, necrosis, and especially acinar cell vacuolization) were more pronounced than in the wild type (Figure 11A), but this was primarily due to the severe basal pancreatic damage in LAMP-2 null mice. The magnitude of

the key pathologic responses caused by LAMP-2 deficiency per se—necrosis, apoptosis (i.e., caspase-3 activation), and macrophage infiltration—was similar to, or even greater than, that induced by CR in wild-type pancreas (Figure 11). Furthermore, the effects of LAMP-2 knockout and CR (relative to wild-type control) were not additive (Figure 11B, E, G, and H), indicating overlapping mechanisms. CR-induced trypsin activity, a hallmark pathologic response, was 4.2-fold in the wild type but only 3.1-fold in the LAMP-2 null pancreas (Figure 11C).

The serum amylase increase was similar in wild-type and LAMP-2 null mice with CR pancreatitis (Figure 11D); however, the fact that pancreatic amylase content is markedly decreased in LAMP-2 null mice (Figure 10A) complicates interpretation of these data. Of note, the pattern of
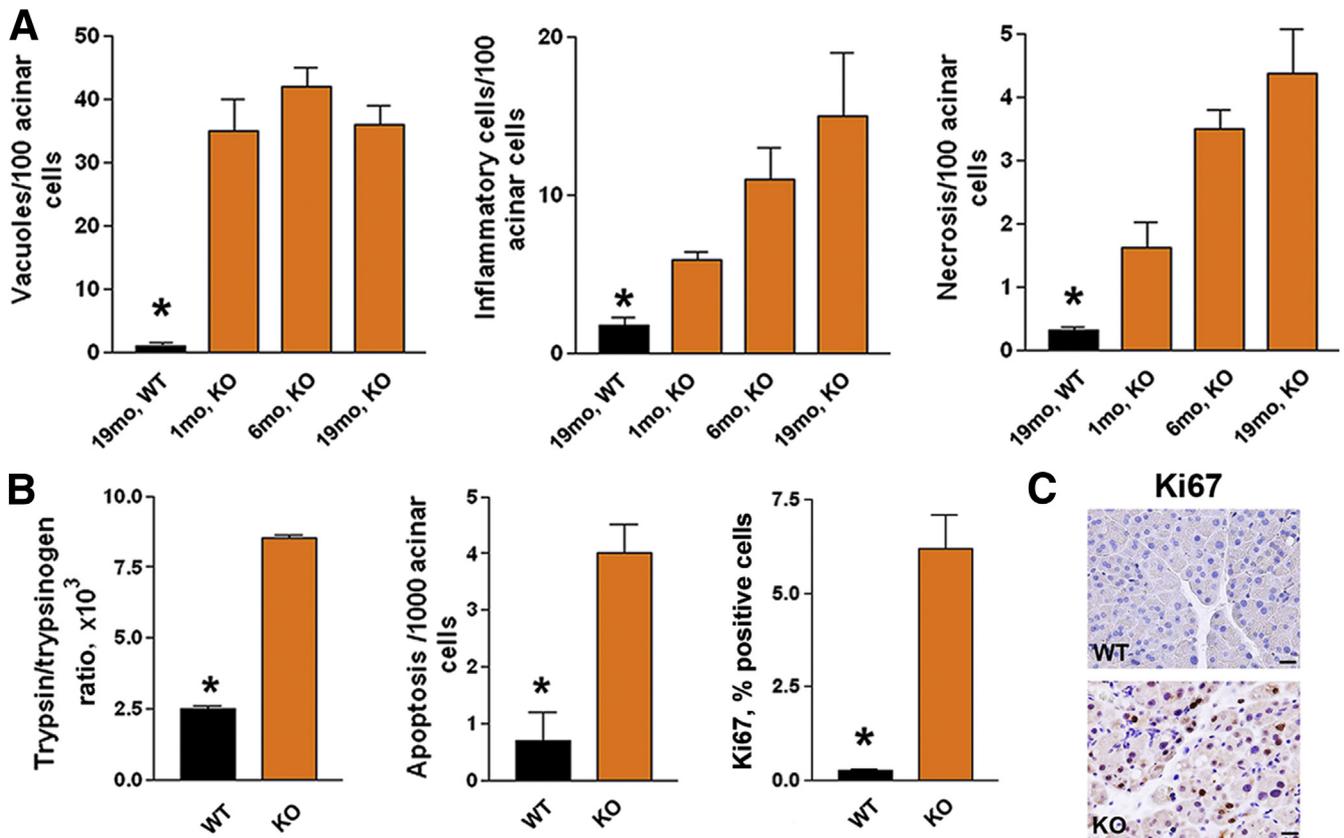
Figure 8. Lysosome-associated membrane protein 2 (LAMP-2)–deficient mice spontaneously develop pancreatitis. Pancreatitis responses were measured in LAMP-2 null mice (knockout) at (*A*) indicated age or (*B*, *C*) 6 months of age. Values are mean ± SEM from at least three mice in each group. *$P < .05$ versus all other groups. Scale bar: 20 μm.

CR-induced inflammatory cell infiltrate differs between the wild-type and LAMP-2 null pancreas. Compared to the wild type, the LAMP-2 null mice with CR pancreatitis displayed greater macrophage infiltration identified by CD68 and CD206 markers (Figure 11*G* and *H*). In contrast, recruitment of neutrophils was inhibited, as evidenced by ∼50% lesser MPO activity (Figure 11*F*). Thus, the inflammatory response of CR pancreatitis in LAMP-2 null mice is shifted toward that of chronic disease. The results in Figure 11 show that, overall, CR-induced responses are blunted in LAMP-2 null mice (as compared with the wild type).

Discussion

LAMPs are critical to the function of lysosomes.[15] We found marked decreases in both LAMP-1 and LAMP-2 in five different rat and mouse models of pancreatitis, the ex vivo model of hyperstimulated acinar cells, and in human pancreatitis. In addition, the LAMP decrease has been observed in ethanol + lipopolysaccharide model of alcoholic pancreatitis.[7] Same as in the normal pancreas, LAMPs in pancreatitis localize to lysosomes and autolysosomes, but in pancreatitis their levels in lysosomes are greatly decreased. There is no such decrease in LIMP-2, a member of a different family of lysosomal membrane proteins, indicating a specific effect of pancreatitis on LAMPs.

Our results are evidence against LAMPs' bulk deglycosylation as the mechanism underlying their decrease in pancreatitis. Instead, the results indicate that pancreatitis causes the degradation of LAMPs, which involves CatB-mediated cleavage of the luminal part of LAMP molecule close to the transmembrane domain. This conclusion is supported by several lines of evidence: 1) comparative immunoblot analysis using C-terminal versus luminal Abs, 2) the absence of pancreatitis-induced LAMP decrease in CatB-deficient mice, and 3) MS analysis of in vitro CatB cleavage of recombinant LAMP-1.

In normal conditions, LAMPs in the lysosome are protected from cleavage by acid hydrolases. One mechanism mediating this protection is that LAMP molecule is heavily glycosylated;[15,17,30] another mechanism is that hydrolases are normally present in the lumen as large multiprotein complexes spatially separated from LAMPs.[42,43] We have shown[6,8] that experimental pancreatitis causes alterations in CatB processing/maturation, resulting in a decrease in its fully mature form and concomitant accumulation of the intermediate and pro-forms. One may speculate that in pancreatitis the abnormal maturation of cathepsins (e.g., altered balance between single- versus double-chain active CatB forms[44]) affects their localization in the lumen and interactions with other lysosomal proteins, resulting in CatB-mediated cleavage of LAMPs. This renders LAMPs
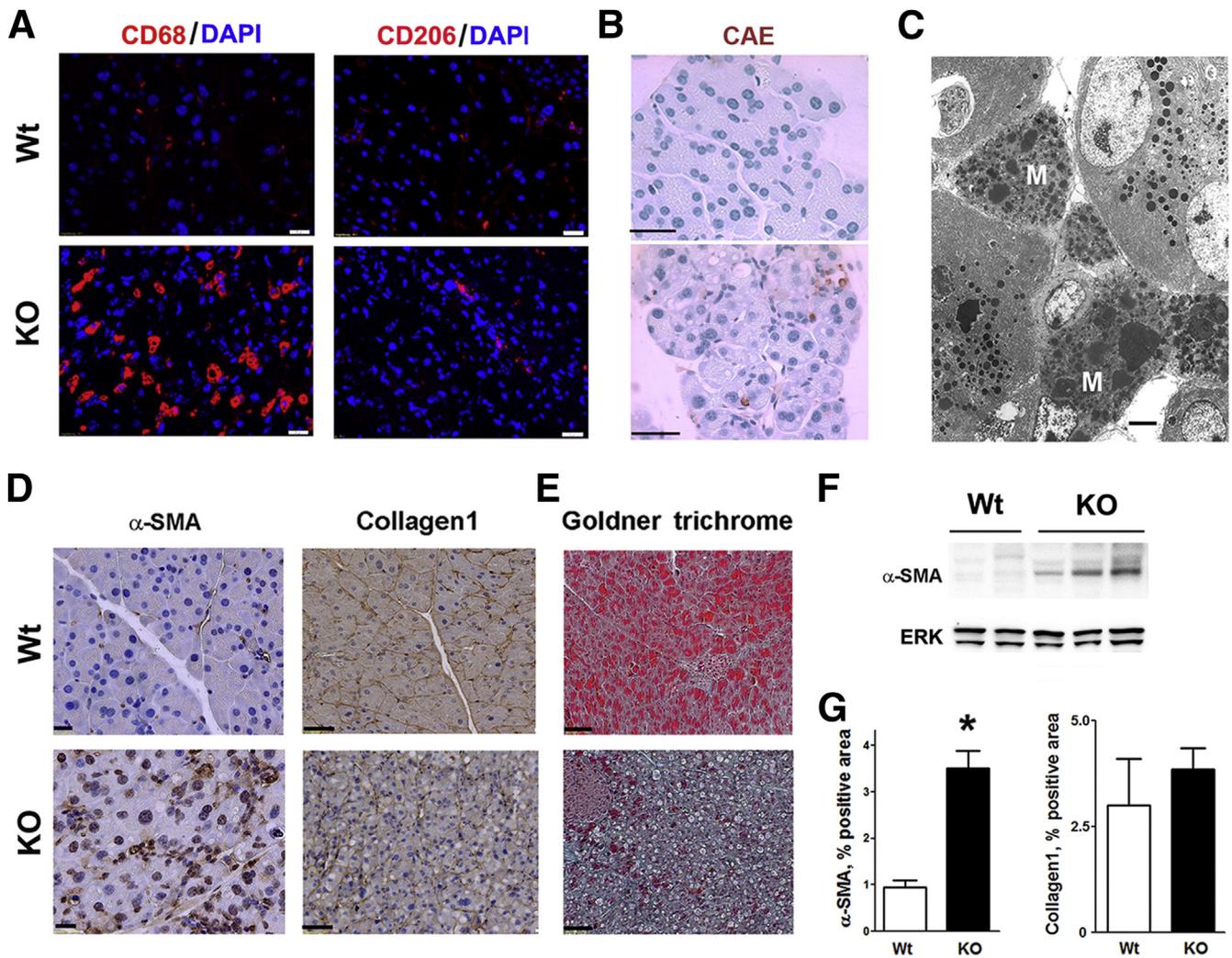
Figure 9. Lysosome-associated membrane protein 2 (LAMP-2) deficiency causes macrophage infiltration and stellate cell activation but not fibrosis in pancreas. Immunofluorescent (*A*), histochemical (*B*, *E*), and immunohistochemical (*D*) staining of pancreatic tissue sections from 6-month-old wild-type and LAMP-2 knockout mice for markers of macrophages (CD68 and CD206), neutrophils [chloroacetate esterase (CAE)], activated stellate cells (α-SMA), and fibrosis (Goldner trichrome and collagen-1). In (*A*), nuclei stained with 4′,6-diamidino-2-phenylindole (DAPI). (*C*). Electron micrograph showing abundant macrophages (M) in pancreas of a 6-month-old LAMP-2 knockout mouse. (*F*) Immunoblot of α-SMA (α-smooth muscle actin) in pancreas of wild-type and LAMP-2 knockout mice. (*G*). α-SMA and collagen-1 were quantified on pancreatic tissue sections as the percentage of the positive area. Values are mean ± SEM (n = 3 per group). *$P < .05$ versus wild type. Scale bars: 10 μm (*A*, *B*, *D*, *E*) and 2 μm (*C*).

unrecognizable by C-terminal Abs. It is likely that other protease(s) work in concert with CatB to cause LAMP degradation in pancreatitis, as is the case in CatA-mediated degradation of LAMP-2a.[32,33] However, the site-specific action of CatB is critical for LAMP degradation, as pancreatitis causes no decrease in LAMPs in CatB-deficient mice.

The role of CatB as a key mediator of the pathologic, intra-acinar trypsinogen activation in pancreatitis is well established.[6,23,26,34] Our results reveal another mechanism through which alterations in CatB may lead to pancreas damage, namely, through LAMP degradation.

LAMP-2 deficiency causes accumulation of large autophagic vacuoles in several organs and results in cardiomyopathy, representing a mouse model of Danon disease.[14,18]

Differently, mice deficient in LAMP-1 do not develop overt pathologic changes, likely because of compensatory LAMP-2 upregulation. In this regard, it is noteworthy that pancreatitis causes marked decreases in both LAMP-1 and LAMP-2.

Although vacuole accumulation has been reported in pancreas of LAMP-2 null mice,[18] the consequences of LAMP deficiency for exocrine pancreas have not been explored. Here, we find that LAMP-2 null mice progressively develop major responses of pancreatitis. Our data indicate that LAMP-2 deficiency primarily targets the exocrine compartment, as LAMP-2 null islets do not exhibit vacuolization or other histopathologic alterations. Autophagy impairment is the earliest pathologic response, already prominent in acinar cells of 1-month-old LAMP-2 null mice by
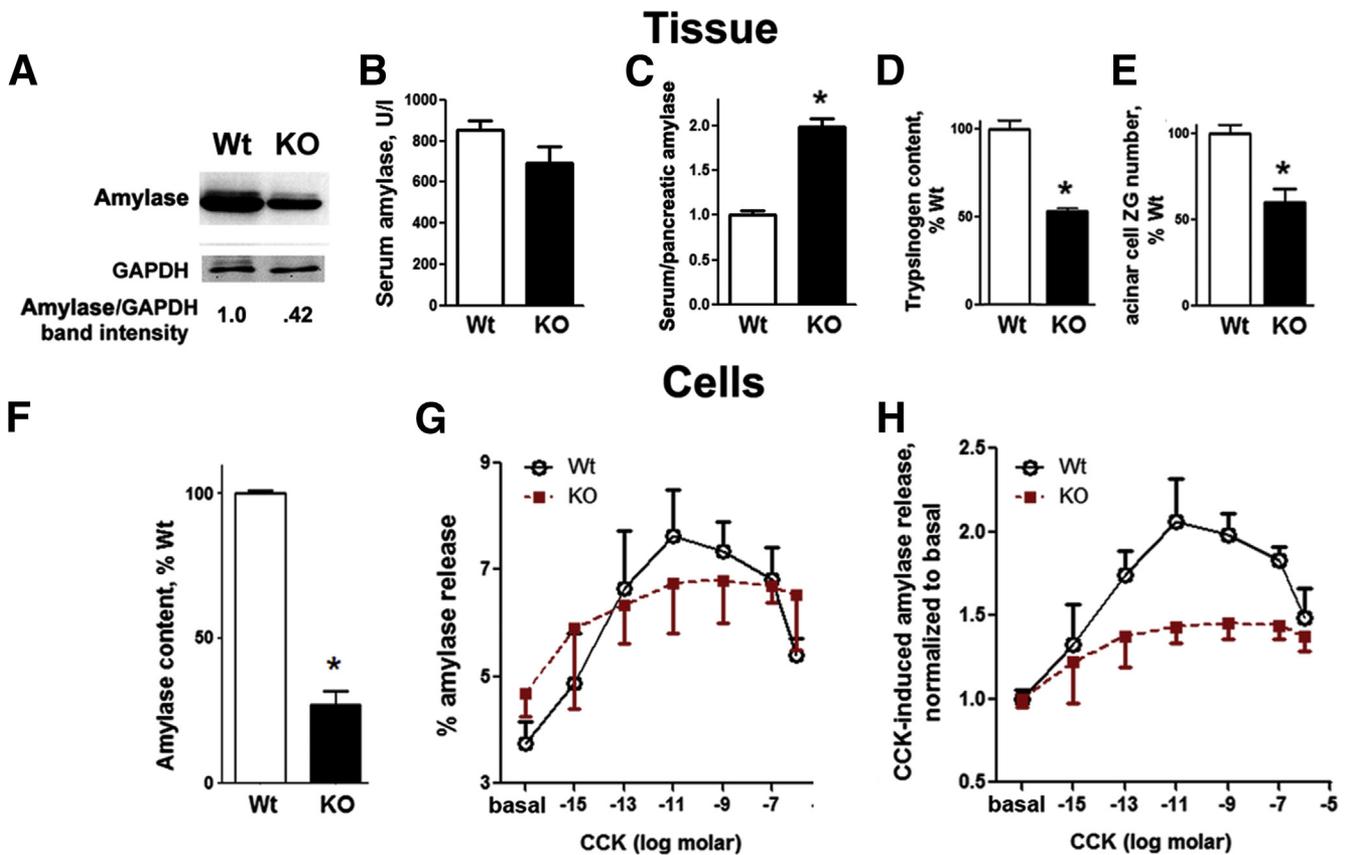
Figure 10. Lysosome-associated membrane protein 2 (LAMP-2) maintains acinar cell homeostasis. (*A–E*). Intrapancreatic content of (*A*) amylase (immunoblot) and (*D*) trypsinogen [enterokinase assay (see *Materials and Methods*)], (*B*) serum amylase level, and (*C*) ratio to intrapancreatic amylase, and acinar cell zymogen granules (ZG) number (*E*) were measured in 6-month-old wild-type and LAMP-2 knockout mice. (*E*) The average ZG number per acinar cell was quantified on electron micrographs of pancreatic tissue sections. (*F–H*) Intracellular amylase content (*F*), and the basal and cholecystokinin (CCK)-induced amylase release (*G, H*) were measured in pancreatic acini isolated from wild-type and LAMP-2 knockout mice and incubated for 30 minutes with and without CCK-8 at indicated concentrations. (*H*) Amylase release from wild-type or knockout mice was normalized to that in the absence of CCK. Values are mean ± SEM; n = 3–4 mice of each genotype (*B–D*), 10–12 cells per group (*E*), 3–4 acinar cell preparations per group (*F–H*). *$P < .05$ versus wild type.

accumulation of large autolysosomes containing poorly degraded cargo. Defective autophagic flux is also manifested by increases in both LC3-II and p62. By the age of 6 months, LAMP-2 null mice develop severe pancreatic damage characterized by tissue disorganization, acinar cell necrosis and apoptosis, massive macrophage infiltration, and stellate cell activation (i.e., α-SMA up-regulation). These pathologic responses are characteristic of chronic pancreatitis; however, despite stellate cell activation LAMP-2-deficient mice do not develop pancreatic fibrosis. One reason for this could be inhibition of autophagy in LAMP-deficient pancreatic stellate cells. Autophagy provides a critical source of energy necessary for activated stellate cells to produce extracellular matrix proteins,[45] and blockade of autophagy in hepatic stellate cells was recently shown to reduce liver fibrogenesis and matrix deposition in experimental hepatitis models.[41] Further studies are needed to determine the role of lysosomes and autophagy in pancreatic stellate cells for the development of fibrosing response of pancreatitis. Another underlying mechanism could be the predominance

of M1 macrophages versus the profibrogenic M2 macrophages in LAMP-2 null pancreas.

LAMP-2 deficiency causes a marked decrease in pancreatic amylase and trypsinogen content; furthermore, it increases the basal and inhibits the CCK-induced amylase release from acinar cells. The results reveal a major role for LAMP-2—more broadly, normal lysosomal/autophagic pathways—in regulating digestive enzyme secretion, the main function of exocrine pancreas.

To determine whether LAMP deficiency makes pancreas more susceptible to acute insult, we subjected LAMP-2 null mice to one episode of CR pancreatitis. Overall, our results indicate that chronic pancreas damage blunts the effects of acute pancreatitis, which correlates with clinical data.[46,47] Most of CR-induced responses in LAMP-2 null mice are "muted," as compared to the wild type. In particular, the effects of LAMP-2 knockout per se and CR on acinar cell vacuolization, necrosis, apoptosis are not additive (relative to wild-type control). Such overlap supports the notion of a pathogenic role of a LAMP decrease in CR-induced and other
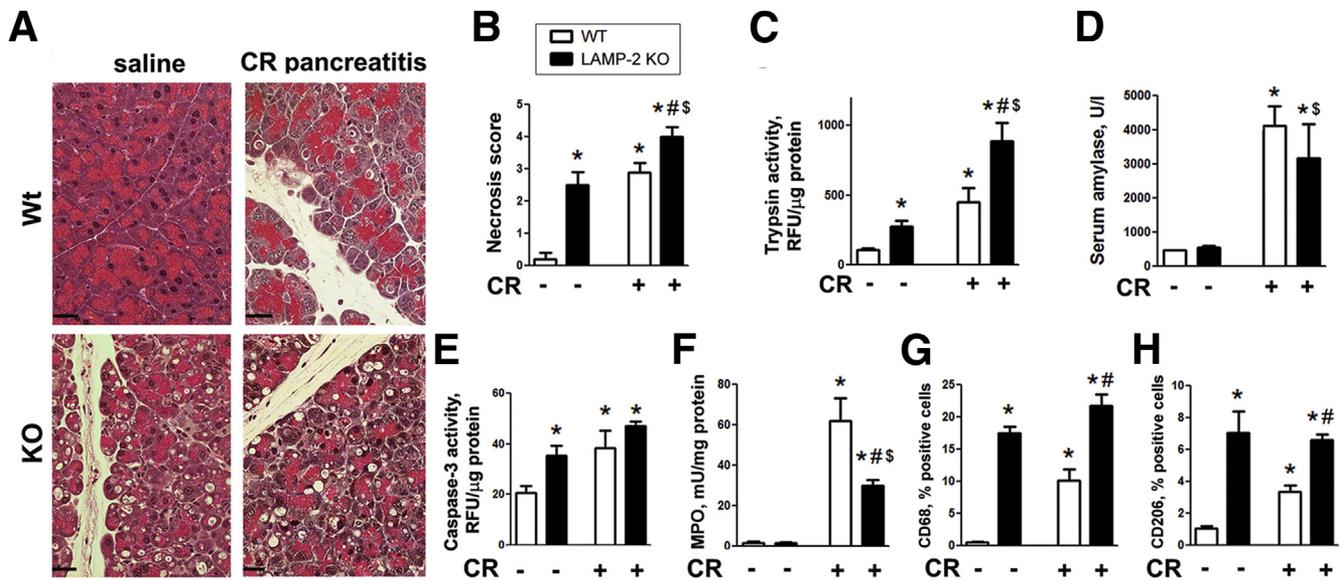
Figure 11. Effects of lysosome-associated membrane protein (LAMP) deficiency on acute cerulein (CR) pancreatitis responses. CR pancreatitis was induced as described in *Materials and Methods*. Histopathologic changes (*A*; H&E staining) and other parameters of pancreatitis were measured in pancreata (*A, C–H*) and serum (*B*) of wild-type and LAMP-2 knockout mice. MPO, myeloperoxidase. Values are mean $\pm$ SEM from 3–4 mice per group. *$P < .05$ versus wild-type saline control; #$P < .05$ versus wild-type CR; $$P < .05$ versus LAMP-2 knockout saline control.

experimental models of pancreatitis (as well as in human disease). Of note, trypsin activity in LAMP-2 null pancreas is further increased by CR, indicating the involvement of LAMP-2 independent mechanism(s). One such likely mechanism, mediating trypsinogen activation, is the aberrant (global and sustained) Ca^{2+} signal.[34] Also noteworthy is the suppression of neutrophilic infiltration in CR-treated LAMP-2 null mice, indicating a shift toward macrophage-driven, "chronic" inflammatory response.

In sum, our results show that lysosomal dysfunction, manifest by LAMP degradation, is a common event in various experimental models and human pancreatitis. Further, LAMP-2 is critical to acinar cell function, and its genetic ablation causes impaired autophagy and the development of pancreatitis. A recent study (published after the submission of this report) showed that pancreas-specific genetic ablation of the key autophagy mediator Atg5 causes spontaneous pancreatitis.[48,49] However, no decrease (or inactivating mutation) in Atg5 has been detected in human disease. Differently, LAMP-2 pancreatic level is greatly decreased in human pancreatitis. It has also been reported[50] that pancreas-specific ablation of the inhibitor of κB kinase α (IKKα), a component of the IKK kinase complex responsible for nuclear factor κB (NF-κB) activation, causes acinar cell damage progressing from vacuole accumulation to chronic pancreatitis. This effect is unrelated to NF-κB; instead, IKKα deficiency impairs the completion of autophagy in acinar cell.[50] In accord with these findings, our study supports the notion[8,9] that disordering of lysosomal and autophagic pathways is a key pathogenic mechanism initiating and driving pancreatitis. Further, it provides evidence that decrease/degradation of LAMPs, particularly LAMP-2, plays an important role in this mechanism. The

new genetic model of pancreatitis caused by LAMP-2 deficiency will help us to understand why the exocrine pancreas is particularly malleable to lysosomal and autophagy dysfunctions as well as to elucidate the mechanisms that link these dysfunctions to pancreatitis pathologies.

References

1. Peery AF, Dellon ES, Lund J, et al. Burden of gastrointestinal disease in the United States: 2012 update. Gastroenterology 2012;143:1179–1187.
2. Pandol SJ, Saluja AK, Imrie CW, et al. Acute pancreatitis: bench to the bedside [erratum 133:1056]. Gastroenterology 2007;132:1127–1151.
3. Aho HJ, Nevalainen TJ, Havia VT, et al. Human acute pancreatitis: a light and electron microscopic study. Acta Pathol Microbiol Immunol Scand A 1982;90:367–373.
4. Helin H, Mero M, Markkula H, et al. Pancreatic acinar ultrastructure in human acute pancreatitis. Virchows Arch A Pathol Anat Histol 1980;387:259–270.
5. Watanabe O, Baccino FM, Steer ML, et al. Supramaximal caerulein stimulation and ultrastructure of rat pancreatic acinar cell: early morphological changes during development of experimental pancreatitis. Am J Physiol 1984;246:G457–G467.
6. Mareninova OA, Hermann K, French SW, et al. Impaired autophagic flux mediates acinar cell vacuole formation and trypsinogen activation in rodent models of acute pancreatitis. J Clin Invest 2009;119:3340–3355.
7. Fortunato F, Burgers H, Bergmann F, et al. Impaired autolysosome formation correlates with Lamp-2 depletion: role of apoptosis, autophagy, and necrosis in pancreatitis. Gastroenterology 2009;137:350–360. e1–5.

8. Gukovskaya AS, Gukovsky I. Autophagy and pancreatitis. Am J Physiol Gastrointest Liver Physiol 2012; 303:G993–G1003.

9. Gukovsky I, Li N, Todoric J, et al. Inflammation, autophagy, and obesity: common features in the pathogenesis of pancreatitis and pancreatic cancer. Gastroenterology 2013;144:1199–1209.e4.

10. Parzych KR, Klionsky DJ. An overview of autophagy: morphology, mechanism, and regulation. Antioxid Redox Signal 2014;20:460–473.

11. Feng Y, He D, Yao Z, et al. The machinery of macroautophagy. Cell Res 2014;24:24–41.

12. Levine B, Kroemer G. Autophagy in the pathogenesis of disease. Cell 2008;132:27–42.

13. Hashimoto D, Ohmuraya M, Hirota M, et al. Involvement of autophagy in trypsinogen activation within the pancreatic acinar cells. J Cell Biol 2008;181:1065–1072.

14. Eskelinen EL. Roles of LAMP-1 and LAMP-2 in lysosome biogenesis and autophagy. Mol Aspects Med 2006; 27:495–502.

15. Saftig P, Klumperman J. Lysosome biogenesis and lysosomal membrane proteins: trafficking meets function. Nat Rev Mol Cell Biol 2009;10:623–635.

16. Wilke S, Krausze J, Bussow K. Crystal structure of the conserved domain of the DC lysosomal associated membrane protein: implications for the lysosomal glycocalyx. BMC Biol 2012;10:62.

17. Fukuda M. Lysosomal membrane glycoproteins. Structure, biosynthesis, and intracellular trafficking. J Biol Chem 1991;266:21327–21330.

18. Tanaka Y, Guhde G, Suter A, et al. Accumulation of autophagic vacuoles and cardiomyopathy in LAMP-2-deficient mice. Nature 2000;406:902–906.

19. Huynh KK, Eskelinen EL, Scott CC, et al. LAMP proteins are required for fusion of lysosomes with phagosomes. EMBO J 2007;26:313–324.

20. Cuervo AM, Dice JF. A receptor for the selective uptake and degradation of proteins by lysosomes. Science 1996;273:501–503.

21. Mareninova OA, Sung KF, Hong P, et al. Cell death in pancreatitis: caspases protect from necrotizing pancreatitis. J Biol Chem 2006;281:3370–3381.

22. Sung KF, Odinokova IV, Mareninova OA, et al. Prosurvival Bcl-2 proteins stabilize pancreatic mitochondria and protect against necrosis in experimental pancreatitis. Exp Cell Res 2009;315:1975–1989.

23. Wartmann T, Mayerle J, Kahne T, et al. Cathepsin L inactivates human trypsinogen, whereas cathepsin L-deletion reduces the severity of pancreatitis in mice. Gastroenterology 2010;138:726–737.

24. Sendler M, Beyer G, Mahajan UM, et al. Complement component 5 mediates development of fibrosis, via activation of stellate cells, in 2 mouse models of chronic pancreatitis. Gastroenterology 2015. Published online. http://dx.doi.org/10.1053/j.gastro.2015.05.012

25. Pandol SJ, Periskic S, Gukovsky I, et al. Ethanol diet increases the sensitivity of rats to pancreatitis induced by cholecystokinin octapeptide. Gastroenterology 1999; 117:706–716.

26. Halangk W, Lerch MM, Brandt-Nedelev B, et al. Role of cathepsin B in intracellular trypsinogen activation and the onset of acute pancreatitis. J Clin Invest 2000;106:773–781.

27. Weng N, Baumler MD, Thomas DD, et al. Functional role of J domain of cysteine string protein in Ca^{2+}-dependent secretion from acinar cells. Am J Physiol Gastrointest Liver Physiol 2009;296:G1030–G1039.

28. Yamada H, Hayashi H, Natori Y. A simple procedure for the isolation of highly purified lysosomes from normal rat liver. J Biochem 1984;95:1155–1160.

29. Slot JW, Geuze HJ. Cryosectioning and immunolabeling. Nat Protoc 2007;2:2480–2491.

30. Kundra R, Kornfeld S. Asparagine-linked oligosaccharides protect Lamp-1 and Lamp-2 from intracellular proteolysis. J Biol Chem 1999;274:31039–31046.

31. Helenius A, Aebi M. Intracellular functions of N-linked glycans. Science 2001;291:2364–2369.

32. Cuervo AM, Dice JF. Regulation of LAMP2a levels in the lysosomal membrane. Traffic 2000;1:570–583.

33. Cuervo AM, Mann L, Bonten EJ, et al. Cathepsin A regulates chaperone-mediated autophagy through cleavage of the lysosomal receptor. EMBO J 2003;22:47–59.

34. Saluja AK, Lerch MM, Phillips PA, Dudeja V. Why does pancreatic overstimulation cause pancreatitis? Annu Rev Physiol 2007;69:249–269.

35. Hietaranta AJ, Saluja AK, Bhagat L, et al. Relationship between NF-κB and trypsinogen activation in rat pancreas after supramaximal caerulein stimulation. Biochem Biophys Res Commun 2001;280:388–395.

36. Verspurten J, Gevaert K, Declercq W, et al. SitePredicting the cleavage of proteinase substrates. Trends Biochem Sci 2009;34:319–323.

37. Mizushima N, Yoshimori T, Ohsumi Y. The role of Atg proteins in autophagosome formation. Annu Rev Cell Dev Biol 2011;27:107–132.

38. Klionsky DJ, Abdalla FC, Abeliovich H, et al. Guidelines for the use and interpretation of assays for monitoring autophagy. Autophagy 2012;8:445–544.

39. Johansen T, Lamark T. Selective autophagy mediated by autophagic adapter proteins. Autophagy 2011;7:279–296.

40. Novak ML, Koh TJ. Macrophage phenotypes during tissue repair. J Leukoc Biol 2013;93:875–881.

41. Hernandez-Gea V, Ghiassi-Nejad Z, Rozenfeld R, et al. Autophagy releases lipid that promotes fibrogenesis by activated hepatic stellate cells in mice and in human tissues. Gastroenterology 2012;142:938–946.

42. Bonten EJ, Annunziata I, d'Azzo A. Lysosomal multienzyme complex: pros and cons of working together. Cell Mol Life Sci 2014;71:2017–2032.

43. Kreutzer R, Kreutzer M, Sewell AC, et al. Impact of beta-galactosidase mutations on the expression of the canine lysosomal multienzyme complex. Biochim Biophys Acta 2009;1792:982–987.

44. Turk V, Stoka V, Vasiljeva O, et al. Cysteine cathepsins: from structure, function and regulation to new frontiers. Biochim Biophys Acta 2012;1824:68–88.

45. Mallat A, Lodder J, Teixeira-Clerc F, et al. Autophagy: a multifaceted partner in liver fibrosis. Biomed Res Int 2014;2014:869390.

46. Akshintala VS, Hutfless SM, Yadav D, et al. A population-based study of severity in patients with acute on chronic pancreatitis. Pancreas 2013;42: 1245–1250.

47. Yadav D, Lowenfels AB. Trends in the epidemiology of the first attack of acute pancreatitis: a systematic review. Pancreas 2006;33:323–330.

48. Diakopoulos KN, Lesina M, Wormann S, et al. Impaired autophagy induces chronic atrophic pancreatitis in mice via sex- and nutrition-dependent processes. Gastroenterology 2015;148:626–638.e17.

49. Gukovsky I, Gukovskaya AS. Impaired autophagy triggers chronic pancreatitis: lessons from pancreas-specific atg5 knockout mice. Gastroenterology 2015; 148:501–505.

50. Li N, Wu X, Holzer RG, Lee JH, et al. Loss of acinar cell IKKalpha triggers spontaneous pancreatitis in mice. J Clin Invest 2013;123:2231–2243.